APPLICATION OF DENSE OPTICAL FLOW IN FLUID DYNAMICS ANALYSIS OF TUNDISH AND MOLD WATER PHYSICAL MODELS

[1]Andrii PYLYPENKO, [1]Peter DEMETER, [1]Dominik DUBEC, [1]Jaroslav DEMETER, [1]Branislav BUĽKO, [1]Lukáš FOGARAŠ, [1]Slavomír HUBATKA, [1]Peter ŠMIGURA

[1]TUKE - Technical University of Košice, Košice, Slovakia, EU, andrii.pylypenko@tuke.sk

https://doi.org/10.37904/metal.2025.5073

Abstract

In this study, Dense Optical Flow (DOF) was applied to videos of tundish and mold water models to reconstruct 2D velocity fields and flow structures. Two bench tests (air bubbles; salt tracer) show that DOF yields quantitative maps suitable for analysis. Compared with Computational Fluid Dynamics (CFD), DOF provides comparable trends at much lower cost than Particle Image Velocimetry (PIV), enabling rapid datasets for digital twins.

Keywords: Dense optical flow, fluid dynamics, computer vision, computational fluid dynamics, continuous casting

1. INTRODUCTION

Industry 4.0 pushes steelmakers toward digital twins, advanced analytics, and AI-driven optimisation to raise productivity and sustainability [1]. Particle Image Velocimetry (PIV) [2] is accurate but costly and cumbersome for routine experiments. Dense Optical Flow (DOF) offers a non-intrusive, low-cost alternative: by processing video frames, it can reveal velocity fields and coherent flow structures in water models with minimal setup [3].

The goal of this study is to develop and validate a dense optical flow–based workflow that recovers quantitative velocity fields and coherent structures from videos of tundish and mold water models, and to benchmark its accuracy with CFD.

2. DENSE OPTICAL FLOW

Dense Optical Flow (DOF) estimates 2-D motion between successive frames for every pixel by enforcing brightness constancy and spatial smoothness. The Farnebäck method [4] approximates local neighborhoods with quadratic polynomials:

$$f(x) \approx x^T A x + b^T x + c \tag{1}$$

and derives displacement:

$$d = -\frac{1}{2} A_1^{-1}(b_2 - b_1) \tag{2}$$

Multi-scale pyramids capture large motions while remaining robust to noise. Although abrupt discontinuities are slightly smeared, the method is accurate enough for bubble or salt solution tracking in water systems.

3. WATER MODELS OF TUNDISH AND MOLD

Scaled acrylic replicas (geometric scale = 1:2) of a single-strand tundish and mold were operated with 20 °C water, whose kinematic viscosity matches that of 1 600 °C molten steel after Froude scaling. Models permit

direct visualisation of inlet jets, recirculation zones, and residence time, helping engineers eliminate turbulence and dead zones before plant trials.

4. 2D PROJECTION OF REAL-WORLD WATER-BASED SYSTEM

4.1 Geometric Projection

A 3-D particle displaced by $\boldsymbol{d}$ projects to the image plane with error $\boldsymbol{E}$ is shown on **Figure 1**; therefore:

$$v_{true} = \frac{E + d}{\Delta t} \tag{3}$$

where:

v_{true} – real velocity of tracked motion (m/s)

E – reprojection error (m)

d – projection distance (m)

Δt – change in time over object's position (s)

$$v_{projected} = \frac{d}{\Delta t} \tag{4}$$

From Equation 3 and Equation 4 it's noticible that:

$$v_{true} \geq v_{projected} \tag{5}$$

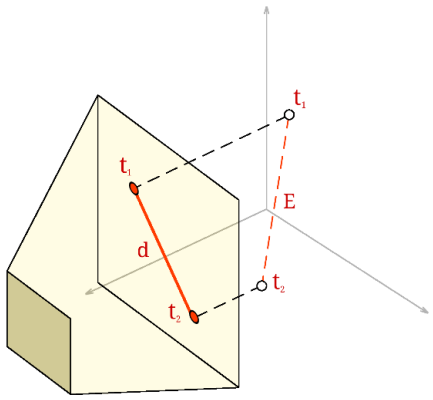

Figure 1 2D projection of 3D space

4.2 Camera Calibration

Camera calibration [5] is a fundamental process in computer vision that aims to determine the intrinsic and extrinsic parameters of a camera to establish a relationship between 3D world coordinates and 2D image coordinates. The first step in camera calibration involves capturing multiple images of a known calibration object, such as a chessboard pattern, from different angles and positions. Those images are processed to identify keypoints, **Figure 2**, that are used for reduction of lens distortion such as barrel or pincushion.

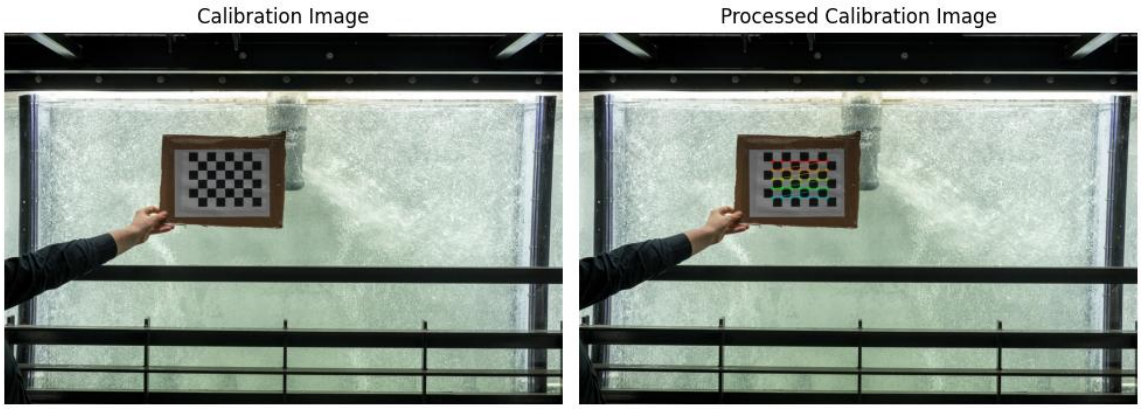

Figure 2 Chessboard keypoints detection for camera calibration

Chessboard images yield the intrinsic matrix, distortion coefficients and extrinsics needed to undistort frames, **Figure 3**, for make pixel to meters calculations more precise. OpenCV [6] python package were used to calculate those parameters.

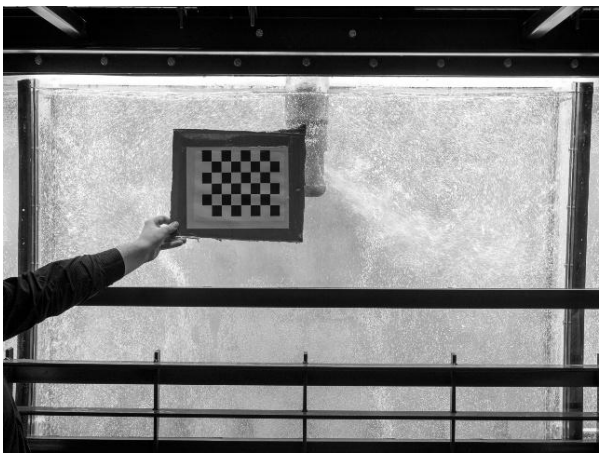

Figure 3 Undistorted frame

4.3 Pixel-to-Metric Conversion

To convert pixel measurements to real-world units, the Field of View (FOV) must first be determined using the following equation:

$$FOV = 2\arctan(\frac{\mathrm{W}}{2\mathrm{FL}}) \tag{6}$$

where:

W – width of sensor (mm)

FL – focal length (mm)

Once the FOV is calculated, the actual width of the scene RW in real-world units can be computed with:

$$RW = 2tan\left(\frac{FOV}{2}\right)D \tag{7}$$

where:

D – distance from sensor to scene (m)

To find the real-world distance per pixel P, the following equation is used:

$$P = \frac{RW}{RES} \tag{8}$$

where:

RES – resolution of camera (pixels)

These calculations enable a precise mapping between pixel-based measurements and real-world dimensions. The next step involves converting motion information from pixel-based measurements p/f where p is displacement of pixels, f is frame to real-world units m/s. This transformation is crucial for accurately analyzing motion in a spatial context beyond the screen. The formula for calculating velocity v in meters per second can be expressed as follows:

$$v = d \times P \times F \tag{9}$$

where:

d – displacement according to Equation 2 (p/f)

P – pixel size (m/p)

F – framerate of video sequence (f/s)

5. EXPERIMENTAL SETUP

Tundish and mold models (transparent acrylic) were filmed at 60 fps. Custom Python code (NumPy, OpenCV) logged images and post-processed DOF fields. Two trials were run:

- **Bubble tracking** – air injection visualised flow in the mold.
- **Salt solution tracer** – highlighted streamlines in the tundish.

6. RESULTS AND EVALUATION

6.1 Bubble speed detection in mold

In **Figure 4**, a processed frame from the experiment is shown.The arrows indicate vectors of detected motion between two frames within a defined motion field. The size and color of each arrow correspond to the speed, with minimum and maximum values indicated in the bottom-left corner of the image. **Figure 5** provides a velocity map that visually represents speed across the water-based model of mold. This map can be instrumental for further analysis in estimating fluid motion over time.

Figure 4 Waterflow speed for 600 l/m incoming water in mold

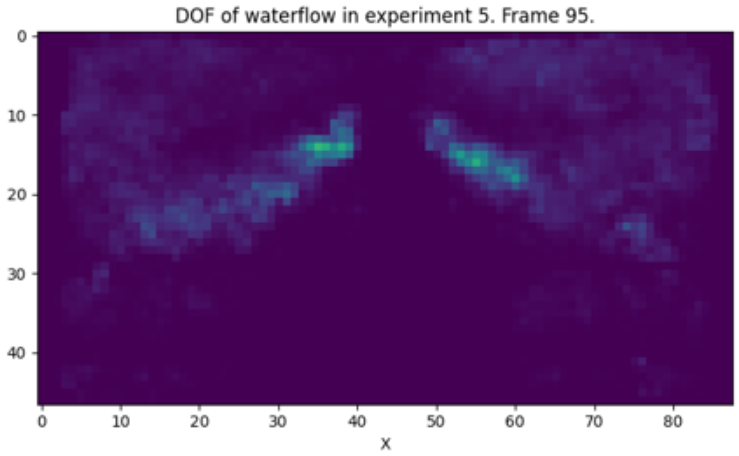

Figure 5 Waterflow speed map for 600 l/m incoming water in mold

6.2 Salt solution detection in tundish

Salt solution flow dynamics within the tundish is illustrated in **Figure 6** and corresponding speed map in **Figure 7**.

Figure 6 Waterflow speed incoming water in tundish

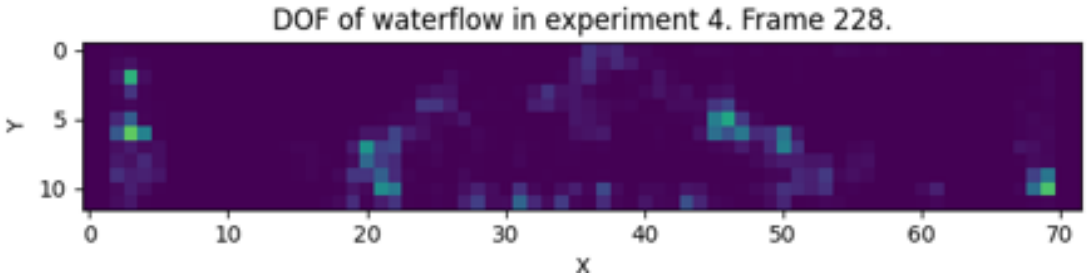

Figure 7 Waterflow speed map incoming water in tundish

6.3 Computational fluid dynamics evaluation

Across both cases Computional Fluid Dynamics (CFD) [7] speeds exceeded DOF by ≈8 %, consistent with 2-D projection theory and minor boundary-condition gaps. Nevertheless, correlation coefficients > 0.9 confirm DOF as a rapid, low-cost alternative to PIV for on-line monitoring or digital-twin data streams. **Figure 8** shows directional correlation for mold within CFD simulation.

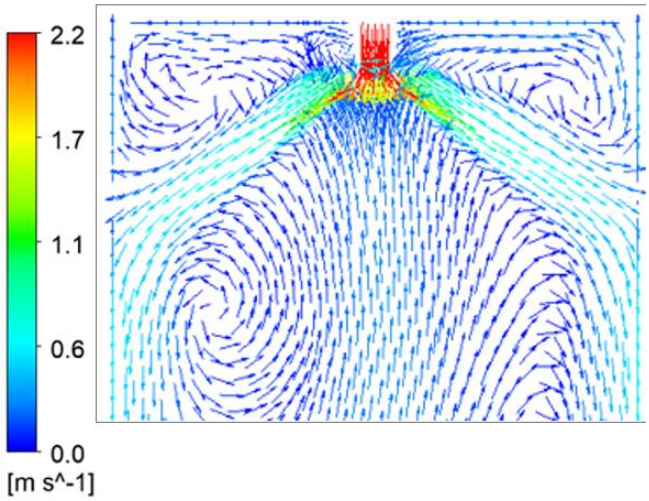

Figure 8 Waterflow vectors of incoming water in mold using CFD Ansys Fluent

7. CONCLUSION

Dense Optical Flow combined with calibrated video of water models offers a scalable, non-intrusive method to characterise steel-casting flow. Agreement with CFD underscores its reliability, while low hardware cost favours deployment in research or plant environments. Future work will extend the approach to machine learning dataset generation about flows and closed-loop control within digital-twin frameworks.

ACKNOWLEDGEMENTS

This research was carried out within the framework of the project APVV-21-0396, with financial support from the Slovak Research and Development Agency (APVV), and was also supported by the VEGA grant No. 1/0335/25. We would like to thank the scientific community and our partners for their valuable assistance and resources.

REFERENCES

[1] MIŚKIEWICZ, R., WOLNIAK, R. Practical application of the Industry 4.0 concept in a steel company. *Sustainability.* 2020, vol. 12, no. 14, p. 5776. DOI 10.3390/su12145776.

[2] RAFFEL, M., et al. Particle Image Velocimetry: A Practical Guide. Cham: Springer, 2018.

[3] WU, H., ZHAO, R., GAN, X., MA, X. Measuring Surface Velocity of Water Flow by Dense Optical Flow Method. *Water.* 2019, no. 11, p. 2320. DOI: 10.3390/w11112320.

[4] FARNEBÄCK, Gunnar. Two-frame motion estimation based on polynomial expansion. In: Image Analysis. Proceedings of the 13th Scandinavian Conference on Image Analysis (SCIA 2003). Gothenburg: Springer, 2003, pp. 363-370.

[5] ZHANG, Z. A Flexible New Technique for Camera Calibration. *IEEE Transactions on Pattern Analysis and Machine Intelligence*. 2000, vol. 22, p. 1330–1334.

[6] BRADSKI, G. The OpenCV Library. *Dr. Dobb's Journal of Software Tools.* 2000, vol. 25.

[7] TKADLEČKOVÁ, M., MICHALEK, K., STROUHALOVÁ, M., SVIŽELOVÁ, J., SATERNUS, M., PIEPRZYCA, J., MERDER, T. Evaluation of Approaches of Numerical Modelling of Solidification of Continuously Cast Steel Billets. *Archives of Metallurgy and Materials*. 2018, 63(2), p. 1003-1008. DOI: 10.24425/122435. ISSN 1733-3490.